最近の研究から

Theoretical studies on photoemission spectra of electron-phonon coupled systems

Kai Ji
Institute of Materials Structure Science

1. Introduction

It has been a long-standing question in solid state physics, how the interplay between electrons and phonons (quanta of lattice vibration) influences the electronic energy band structures, and finally determines a material to become an insulator, metal or superconductor. Since the angle resolved photoemission spectra (ARPES) can directly probe the structure of electronic energy bands and topology of Fermi surface, it has become one of the most important measurements for the experimental studies [1]. With the rapid development of high resolution ARPES, nowadays the electronic energy band structure can be discerned in the scale of a few meV. Based on this technical improvement, quite a lot of new properties associated with electron-phonon (e-ph) interaction have been discovered in the normal metallic states as well as in the superconducting ones [2-7], signifying direct and clear evidences for the importance of the e-ph interactions.

According to recent experimental results, it has become clear that the ARPES evolve quite drastically as the momentum changes from the Fermi momentum ($\equiv p_F$) to the bottom of valence band. As shown in Fig. 1, the ARPES on Be(0001) surface [2-4] take sharp two-headed asymmetric Lorentzians at around p_F, while become broad Gaussian at around the band bottom. Since there was no charge density wave or
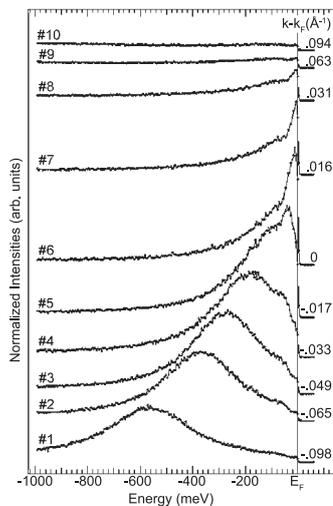
Figure 1 ARPES of the Be(0001) surface state measured at 12 K along the ΓM line of the surface Brillouin zone. [Reprinted figure with permission from Hengsberger, Purdie, *et al.*, Phys. Rev. Lett. **83**, 592, (1999). Copyright (1999) by the American Physical Society.]

superconductivity observed in the experiment, this spectral feature has been attributed to the e-ph interaction. Later, similar spectral evolution was also found in the conduction plane of $Bi_2Sr_2CaCu_2O_8$ [5], which is now believed to be an evidence of strong e-ph interplay in this material. These experiments clearly tell us that the electrons near p_F are in the coherent plane wave states, while, at around the band bottom, they are in the incoherent quasi-localized states. This spectral evolution from the two-headed Lorentzian to the broad Gaussian, or from the coherent state to the incoherent one, is quite universal, and has become a basic problem of the e-ph coupling.

In the theoretical aspect, it is already known that these spectra are nothing, but the Lehmann's representation of the one-body Green's function. So they can be evaluated by various theories. However, the origin for the abovementioned spectral evolution seems beyond the conventional mean field and approximation methods, like the standard Migdal-Eliashberg theory [8,9], which predict only a single peak at p_F and fail to describe such a momentum-dependent evolution. Thus, the problem how e-ph interaction dominates the spectral shape has emerged as a new challenge for the theory of solid state physics.

To clarify the origin for the spectral evolution, in our research, we have developed a new path-integral theory to calculate the ARPES. By applying it to an e-ph coupled model, we have successfully reproduced the spectral change, thus confirm the importance of e-ph interaction in these materials.

2. Model and Methods

To investigate the spectral evolution due to the e-ph interaction, we consider the Holstein model [10]. Its Hamiltonian reads (h = 1),

$$H = -T\sum_{<l,l'>}\sum_{\sigma}\left(a_{l\sigma}^+ a_{l'\sigma} + a_{l'\sigma}^+ a_{l\sigma}\right) - \mu\sum_{l\sigma} n_{l\sigma}$$
$$+ \sum_{l}\left(\frac{P_l^2}{2m} + \frac{1}{2}m\omega_0^2 Q_l^2\right) - S\sum_{l\sigma} Q_l\left(n_{l\sigma} - \frac{\bar{n}}{2}\right),$$

$$n_{l\sigma} \equiv a_{l\sigma}^+ a_{l\sigma}, \quad \sigma = \alpha \text{ or } \beta, \quad \bar{n} \equiv N_e / N. \qquad (1)$$

Here $a_{l\sigma}^+$ and $a_{l\sigma}$ are the creation and annihilation operators for the conduction electron with spin σ at site l. The total number of sites in a lattice is N, while the total electron number is N_e, and the average electron number per site is $\bar{n}$. T is the transfer energy,
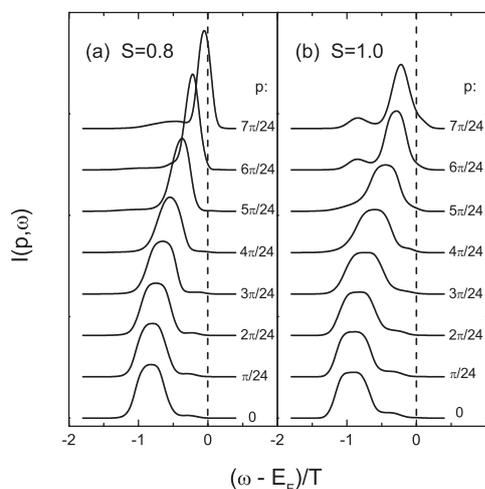
and μ the chemical potential of electrons. In this model, the electrons hop between two nearest neighboring sites, denoted by $<l,l'>$, and couple to the Einstein phonons, which are localized at each site l. P_l and Q_l are the momentum and coordinate operators for this phonon at the site l, with a frequency ω_0 and a mass m. S is the coupling constant of this e-ph interaction.

By using a path integral theory [11,12], we calculate the electronic Green's function [$\equiv G_\sigma (p,\tau)$]. The numerical calculation of this path-integral is performed by the hybrid quantum Monte Carlo (QMC) simulation method [13] with a leap-frog algorithm [14]. And then the electronic spectral function [$\equiv A_\sigma (p,\omega)$] and the spectral intensity [$\equiv I (p,\omega)$] is derived through the analytic continuation [15,16].

3. Comparison with Experimental Results

In this section, we present our numerical results of spectra for the Holstein models. Since we are mainly interested in the normal or quasi metallic states, we shall restrict our attention to the weak and intermediately coupled e-ph systems with little high temperatures, i.e., $\beta = 20 \sim 25$ in the unit of T. In the typical metallic systems due to 3d or 2p electrons, the full bandwidth of electron is 2 eV or so [17]. For the phonon, its energy is usually of the order of 0.1 eV or less. However, too small ω_0 is not appropriate for the QMC calculation. For this sake, we set T as the unit of energy and the phonon energy $\omega_0 = 0.1$ in the numerical calculations.

In Fig. 2, we show our results of $I(p,\omega)$ of one dimensional (1D) Holstein model at 29.17%-filling (48 sites with 28 electrons) for two different e-ph coupling constants. The panel (a) corresponds to $S = 0.8$, and (b) $S = 1.0$. The inverse temperature is $\beta = 20$. The phonon effective mass is taken as $m = 80$ here. From panel (a) we can see the spectrum takes a broad Gaussian near the band bottom $p = 0$. As p increases, the peak width gradually decreases, and at $p_F = 7\pi / 4$, the spectrum shows a slightly two-headed Lorentzian. In the panel (b), we have

increased S, thus the spectra close to the band bottom are further broadened. While near p_F, a second peak appears, and the whole spectrum has become a two-headed asymmetric Lorentzian. These behaviors are well consistent with the aforementioned experimental discoveries, although the agreement between the theory and the experiments are qualitative.

In Fig. 3, we show our QMC results for the two dimensional (2D) case along the ΓM symmetry line of the Brillouin zone at 35.94%-filling (8×8 square lattice with 46 electrons) for two different coupling constants. The panel (a) is for $S = 0.8$, and (b) is $S = 1.0$. β is same as that of Fig. 2. Although our simulation on the 8×8 system gives us only a limited number of p's, the main feature of the aforementioned spectral evolution is well displayed here. Near the band bottom, the spectra have a broad Gaussian shape, while at p_F, the spectra show an asymmetric Lorentzian form. With the increase of coupling constant, the spectra at p_F change from a slightly two-headed form to a clear two-headed one. These results are in good agreement with the experimental observations.
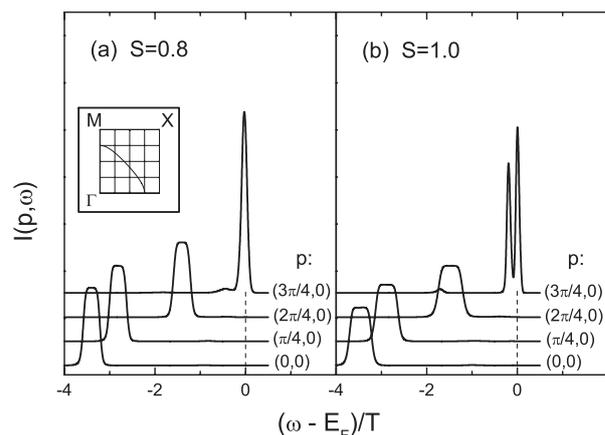
Figure 3 Calculated ARPES of 2D Holstein model at 35.94%-filling (8×8 square lattice with 46 electrons) along the ΓM direction for different e-ph coupling constants S. The inset of (a) shows the Brillouin zone and the Fermi surface.

Figure 2 Calculated ARPES of 1D Holstein model at 29.17%-filling (48 sites with 28 electrons) for different e-ph coupling constants S.
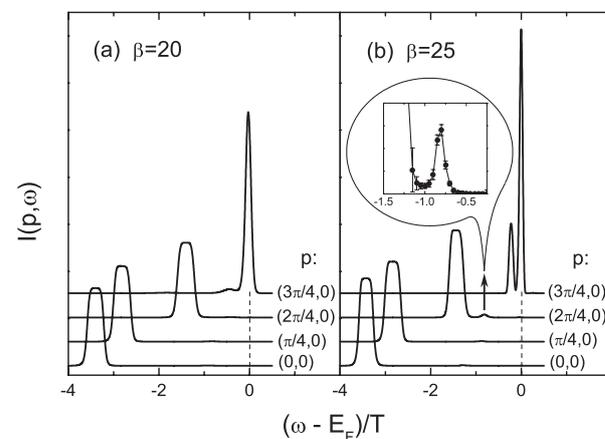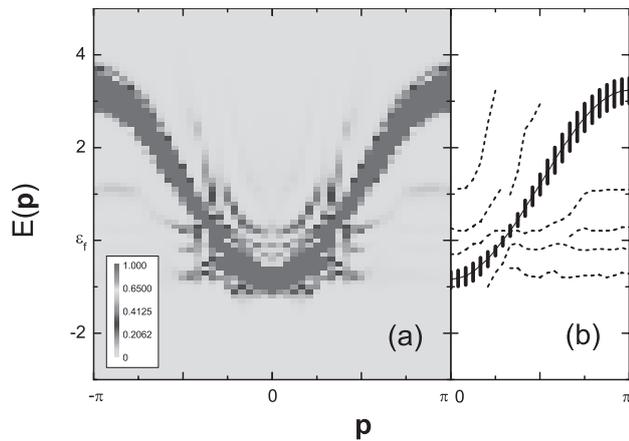

Figure 4 Calculated ARPES of 2D Holstein model at 35.94%-filling (8×8 square lattice with 46 electrons) along the ΓM direction for different temperatures β. The inset magnifies the small hump denoted in (b).

In Fig. 4, the temperature dependence of spectra is presented for the 2D case at 35.94%-filling (8×8 square lattice with 46 electrons). The panel (a) is for $\beta = 20$, and (b) $\beta = 25$. The e-ph coupling constant is fixed at $S = 0.8$. In comparison with Fig. 3, we see, decreasing temperature also brings about a notable phonon peak at p_F. On the other hand, since the thermal broadening is suppressed at low temperature, in the panel (b), the spectral shape becomes narrower and sharper. We can also say that some fine structure, obscured in the panel (a), becomes more pronounced under the low temperature condition (b). For example, a small hump appears in the spectrum $p = 2\pi / 4$. In the inset, we have zoomed to this small peak with clear error bars. Here we can clearly see, these weak structures are not numerical errors, but are other phonon peaks.

4. General Description of Spectral Evolution

If we place the spectral functions $A_\sigma(p,\omega)$ side by side as a function of momentum p, then we get the graph like Fig. 5(a), from which we can know the band structure with ease. In Fig. 5(a) we present the intensity map of 1D Holstein model at 29.17%-filling (48 sites with 28 electrons), with $S = 0.8$, $T = 1.0$, $\omega_0 = 0.1$, $\beta = 20$, $m = 80$. In Fig. 5(b), we show the skeleton image of the energy bands obtained by connecting the peak maxima shown in (a). In the panel (a), we can easily recognize the cosine-shaped main band. In the panel (b), the corresponding structure is denoted by the solid line, and the half-width of the cosine band is schematically shown by the error bars. In addition to the main band, the weak phonon bands can also be seen in the intensity map (a). We outline them by the dash lines in the skeleton image (b).

In these figures, p is nothing but the momentum of the added hole or electron in the N-electron system, and $E(p)$ is the polaron energy. These graphs of band structure can be understood from the view of the recoil effect of the electron [20] (here we confine the interpretation within the case of the hole left under E_F after the photo excitation. Note the hole-phonon interaction is same as the electron-phonon interaction). In the e-ph system, the motions of the electron and phonon are mutually interfered. The motion of the phonons changes the potential field felt by the electron, while the electron also changes the potential exerted on the phonon. As a result, the instaneous status of the electron and phonon is always changing. What we exactly know is only the total polaron momentum p, which is conserved during the e-ph scattering. Hence the spectrum for each momentum p provides us a picture of the entangled electron and phonon, i.e., the polaron.

In the noninteracting limit, no phonon is created or annihilated, and the total polaron energy of momentum p is equivalent to the electronic tight binding energy, $E(p) = \varepsilon_p$. When the e-ph interaction is introduced, the total polaron energy is also changed from ε_p. For example, it becomes $\varepsilon_{p+q} + \omega_{-q}$ after the hole emits a phonon of momentum $-q$ and is recoiled from ε_p to ε_{p+q}. This state may correspond to a new peak at $E(p) = \varepsilon_{p+q} + \omega_{-q}$ away from the main peak at $E(p) = \varepsilon_p$ (see in Figs. 6(a) and 6(b)). One can expect that small energy change due to phonon creation or annihilation only contributes to the broadening of the main band, and dramatic change gives rise to some new phonon bands. If more phonons are involved in this process, the main band (as well as phonon bands) can be further broadened, and more phonon bands can be formed.

The energy difference of electron due to e-ph scattering can be estimated by $\Delta E = (\partial E(p)/ \partial p) \Delta p$, where Δp comes from the momentum exchange with phonon. For the case of cosine band, $E(p) \sim -\cos(p)$, so ΔE is small near the band bottom, and the e-ph
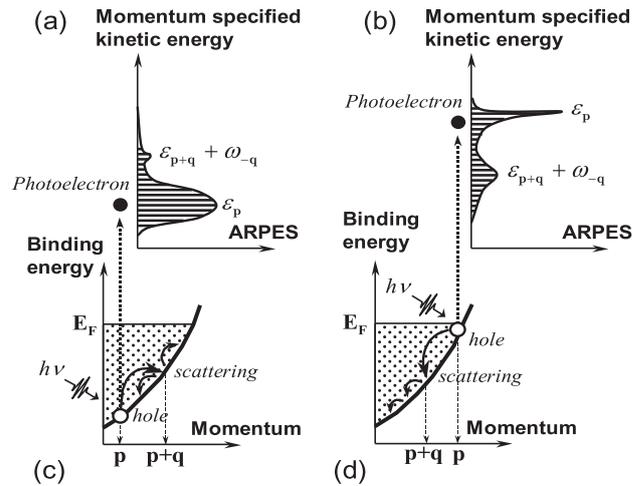

Figure 5 Band structure of 1D Holstein model at 29.17%-filling (48 sites with 28 electrons). Panel (a) is the intensity map of QMC raw data. (b) is the skeleton image of the energy bands obtained by connecting the peak maxima shown in (a). The solid line corresponds to the main band, and the error bars denote its half-width. The phonon bands are shown by the dash lines.

Figure 6 ARPES and the dynamics of multiple scattering in the e-ph coupled system. In the panel (c), a hole is created near the band bottom after the photo excitation, and (d) is the case close to the Fermi surface. The lower panels (c) and (d) show the scattering processes in the electronic band. The upper panels (a) and (b) are the corresponding spectral densities.

scattering mainly contributes to the broadening effect. Some weak phonon peaks can only be seen to the lower energy side of the cosine band (Fig. 6(a)), this is because $\varepsilon_{p+q} + \omega_{-q}$ is always less than ε_p (allowing for that in the normal state, phonon energy ω_q is negligible for the electron). For the scattering near E_F, ΔE can be relatively large, which favors creating new phonon peaks. These peaks, in this case, appear only to the high binding energy side (Fig. 6(b)), since the hole cannot be scattered into the empty band above E_F. The scattering can also occur between E_F and band bottom, and hence the phonon bands above and below the cosine band can both be produced.

A hole just under E_F is the most stable one in the energy band. At that position, the hole can easily settle down without much virtual phonon excitation. So if an electron is excited from somewhere near E_F, its photoemission spectral shape will be almost free-electron-like and take a sharp Lorentzian form (Fig. 6(b)). While, if an electron is excited from the band bottom, the high energy hole left at the band bottom will induce thick phonon cloud around it. As a result, the spectral shape is heavily modified by the e-ph interaction and has a broad Gaussian distribution (Fig. 6(a)). A statistical average over all the procedures described above then give us spectral evolution of ARPES.

5. Summary

In this work, we have developed a path-integral theory to calculate the photoemission spectra of the e-ph coupled systems. We have systematically studied the spectral properties of the e-ph coupled systems based on the 1D and 2D e-ph coupled models under various conditions. We find the band structure is greatly modified by the multiple scattering effect of electron with phonons, even if the whole system is still metallic and the e-ph coupling strength is intermediate. Around the band bottom, the spectrum takes a broad Gaussian, indicating the electron in this state is nearly localized and incoherent. While near the p_F, the spectral shape is characterized by an asymmetric two-headed Lorentzian, which means the electron in this state is almost coherent with a plane wave nature, extending over all the crystal. Our results qualitatively agree with recent experiments of high resolution ARPES.

References

[1] P. Hüfner, *Photoelectron Spectroscopy*, 3rd ed. (Springer, Berlin, 2003).

[2] M. Hengsberger, D. Purdie, P. Segovia, M. Garnier, and Y. Baer, Phys. Rev. Lett. **83**, 592 (1999).

[3] M. Hengsberger, R. Fresard, D. Purdie, P. Segovia, and Y. Baer, Phys. Rev. B **60**, 10796 (1999).

[4] S. LaShell, E. Jensen and T. Balasubramanian, Phys. Rev. B **61**, 2371 (2000).

[5] A. Lanzara , P. V. Bogdanov, X. J. Zhou, S. A. Kellar, D. L. Feng, E. D. Lu, T. Yoshida, H. Eisaki, A. Fujimori, K. Kishio, J. -I. Shimoyama, T. Noda, S. Uchida, Z. Hussain, and Z. -X. Shen,et al., Nature **412**, 510 (2001).

[6] T. Yokoya, T. Kiss, A. Chainani, S. Shin, M. Nohara, H. Takagi, Science **294**, 2518 (2001).

[7] X. J. Zhou, T. Yoshida, A. Lanzara, P. V. Bogdanov, S. A. Kellar, K. M. Shen, W. L. Yang, F. Ronning, T. Sasagawa, T. Kakeshita, T. Noda, H. Eisaki, S. Uchida, C. T. Lin, F. Zhou, J. W. Xiong, W. X. Ti, Z. X. Zhao, A. Fujimori, Z. Hussain, Z. -X. Shen, Nature **423**, 398 (2003).

[8] A. B. Migdal, Sov. Phys. JETP **7**, 996 (1958).

[9] G. M. Eliashberg, Sov. Phys. JETP **11**, 696 (1960).

[10] T. Holstein, Ann. Phys. (N.Y.) **8**, 325 (1959).

[11] K. Nasu, J. Phys. Soc. Jpn. **65**, 2285 (1996).

[12] K. Ji, H. Zheng, and K. Nasu, Phys. Rev. B **70**, 085110 (2004).

[13] S. Duane, A. D. Kennedy, B. J. Pendleton, and D. Roweth, Phys. Lett. B **195**, 216 (1987).

[14] M. P. Allen and D. J. Tildesley, *Computer simulation of liquids* (Clarendon, Oxford, 1987).

[15] S. R. White, D. J. Scalapino, R. L. Sugar, and N. E. Bickers, Phys. Rev. Lett. **63**, 1523 (1989).

[16] J. E. Gubernatis and M. Jarrell, Phys. Rep. **269**, 135 (1996).

[17] K. Nasu, in *Electronic Conduction in Oxides*, edited by N. Tsuda (Springer, Berlin, 1999), Chap. 3.

[18] G. D. Mahan, *Many-particle Physics*, 2nd ed. (Plenum, New York, 1990).

著者紹介
吉凱　Kai JI

物質構造科学研究所　協力研究員
〒 305-0801　茨城県つくば市大穂 1-1
TEL: 029-879-6026
FAX: 029-864-3202
e-mail: jikai@post.kek.jp
略歴：2000 年中国上海交通大学理学院
凝聚態物理専攻卒業，2004 年総合研究
大学院大学数物科学研究科物質構造科学専攻博士課程修
了，2004 年物質構造科学研究所協力研究員。理学博士。
最近の研究：異常同位元素効果と電子・格子系の経路積分
理論